Extension along the Australian-Pacific transpressional transform plate boundary near Macquarie Island

Nathan R. Daczko

Department of Geological Sciences and Institute for Geophysics, Jackson School of Geosciences, University of Texas, Austin, Texas 78712, USA (ndaczko@els.mq.edu.au)

Now at GEMOC ARC National Key Centre, Department of Earth and Planetary Sciences, Macquarie University, NSW 2109, Australia

Karah L. Wertz

Department of Geological Sciences and Institute for Geophysics, Jackson School of Geosciences, University of Texas, Austin, Texas 78712, USA

Geochemistry Division, Max–Planck–Institut für Chemie, Abteilung Geochemie Postfach 3060, D-55020 Mainz, Germany (karah@mail.utexas.edu)

Sharon Mosher

Department of Geological Sciences, Jackson School of Geosciences, University of Texas, Austin, Texas 78712, USA (mosher@mail.utexas.edu)

Millard F. Coffin

Institute for Geophysics, Jackson School of Geosciences, University of Texas, Austin, Texas 78712, USA

Ocean Research Institute, University of Tokyo, 1-15-1 Minamidai, Nakano-ku, Tokyo 164-8639, Japan (mcoffin@ori.u–tokyo.ac.jp)

Tip A. Meckel

Department of Geological Sciences and Institute for Geophysics, Jackson School of Geosciences, University of Texas, Austin, Texas 78712, USA (tameckel@colby.edu)

[1] The Australian-Pacific transform plate boundary fault zone along the Macquarie and McDougall segments of the Macquarie Ridge Complex (MRC), south of New Zealand, is characterized by dominantly normal faults and pull-apart basins, in apparent conflict with the regional transpressional tectonic setting. We propose that present-day curvature of the transform is inherited from a preexisting divergent plate boundary and that the overall extensional kinematics shown by faults along the main plate boundary trace and exposed on Macquarie Island result from local stresses related to right-lateral, right stepping, en echelon plate boundary faults and not to the current transpressional setting. Transpression along the Australian-Pacific transform plate boundary has resulted in uplift along the ~1500 km long Macquarie Ridge Complex. Macquarie Island, the only subaerial exposure of the complex, sits atop a ~5 km high, ~50 km wide submarine ridge of oceanic crust and lies ~4.5 km east of the major active plate boundary fault zone. Thus Macquarie Island and the surrounding seafloor provide a unique opportunity to study an active oceanic transform fault using complementary marine geophysical and land-based geological data. Mapping of recent faults affecting the topography of Macquarie Island shows that the island is extensively cut by high-angle normal faults forming pull-apart basins. Furthermore, evidence for reverse motion is rare. Using marine geophysical data, including swath bathymetry, reflectivity, and seismic reflection data, collected along the Australian-Pacific plate boundary north and south of the island, we have defined a

5–15 km wide plate boundary zone. A series of right stepping en echelon faults, within this zone, lies along the main plate boundary trace. At the right stepping fault terminations, elongate depressions ($\leq$10 km wide and 1.2 km deep) parallel the plate boundary, which we interpret as extensional relay zones or pull-apart basins. We propose that transpression is partitioned into en echelon strike-slip faults at the plate boundary and a convergent component that flexes the crust, causing the anomalous bathymetric ridge and trough morphology of the McDougall and Macquarie segments of the MRC.

1. Introduction

[2] Studies of oceanic transform faults are hindered by limited subaerial exposure. Our knowledge of oceanic transform faults therefore comes from bathymetry and other geophysical data, dredge samples and in a few areas survey and sampling by submersibles [e.g., *Mitchell*, 2000]. Moreover, even where rarely exposed on land within ophiolites, paleo-oceanic transform faults have typically been deformed to varying degrees during obduction [e.g., *Karson*, 1984; *Simonian and Gass*, 1978].

[3] Macquarie Island, located approximately 1200 km southwest of New Zealand in the Southern Ocean (Figure 1), forms the apex of the Macquarie Ridge Complex (MRC), a system of ridges and troughs along the currently active Australian-Pacific oceanic transform plate boundary between the Alpine Fault of New Zealand and the Australian-Pacific-Antarctic triple junction. The island exposes the eastern side of the ~5 km high, ~50 km wide submarine ridge and lies ~4.5 km east of the major active plate boundary fault zone. Macquarie Island represents a globally unique opportunity to examine an active oceanic transform plate boundary as it is the only subaerial exposure of non-plume-related oceanic crust that still lies within the basin in which it formed. Thus oceanic transform

related structures on the island may be placed into a relatively well-constrained present-day plate tectonic setting.

[4] We present field relationships, petrological data and structural analyses of fault geometry, style and kinematics for recent faults on Macquarie Island and examine marine geophysical data including swath and single-beam bathymetry, high-quality reflectivity (acoustic backscatter), and seismic reflection data [*Massell et al.*, 2000; *Bernardel and Symonds*, 2001] across the plate boundary north and south of Macquarie Island. On the basis of these data, we propose a model for the tectonic development of the transform plate boundary, and compare and contrast our results with those from other oceanic transforms and well-studied continental transform plate boundaries.

2. Tectonic Setting

[5] Oceanic crust around Macquarie Island originated at three different seafloor spreading systems, the Southeast Indian, Pacific-Antarctic, and Macquarie (shown stippled in Figure 1) spreading ridges [*Cande et al.*, 2000]. The first two spreading centers are still active, whereas crust of the Macquarie region was generated at the divergent Australian-Pacific plate boundary following break-up between the Campbell Plateau and Resolution
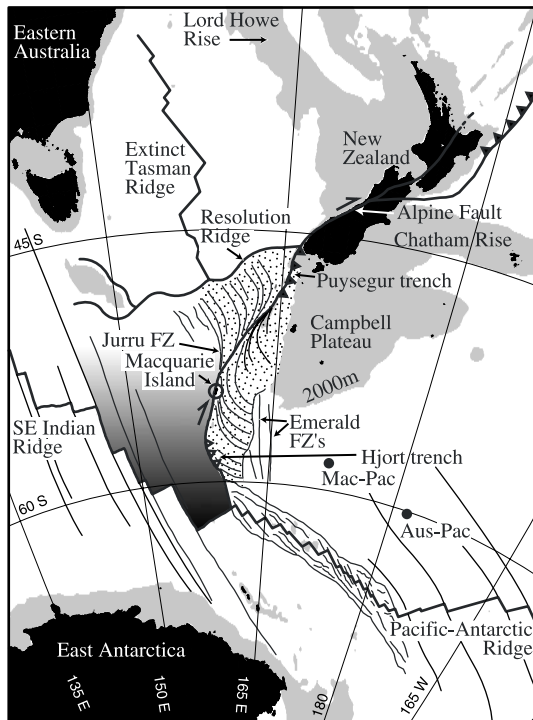
Figure 1. Location map of Macquarie Island and the Australian-Pacific transform plate boundary south of New Zealand (Macquarie Ridge Complex). Crust formed by Australian-Pacific spreading along the Macquarie spreading ridge between ~40 and ~10 Ma is stippled. Gradient shaded crust is the Macquarie plate that formed and began moving independently of the rest of the Australian plate at ~6 Ma (Cande and Stock, submitted manuscript, 2003). Filled triangles along the plate boundary are subduction zones; open triangles in the Hjort region represent incipient subduction (Meckel et al., submitted manuscript, 2003). Light gray illustrates regions of seafloor shallower than 2000 m. The locations of the Australian-Pacific (NUVEL-1A) [*DeMets et al.*, 1994] and the Macquarie-Pacific (2Ay) (Cande and Stock, submitted manuscript, 2003) poles of rotation are indicated by solid circles. Past and present plate boundaries are shown as thick black lines. Fracture zones (FZ) are shown as thin black lines. Azimuthal equidistant projection centered at 60°S, 180°E.

Ridge between middle Eocene (~40 Ma) [*Wood et al.*, 1996] and late Miocene time (Figure 1; ≤10 Ma from the age of Macquarie Island crust) [*Duncan and Varne*, 1988]. Fracture zones in the Macquarie region crust curve and merge asymptotically into the active Australian-Pacific plate boundary (Figures 1 and 2), consistent with progressive clockwise rotation of the spreading axis segments with time [*Massell et al.*, 2000]. The cumulative length

of spreading segments along the plate boundary decreased relative to that of transform faults until spreading ceased at ≤10 Ma. At that time, right lateral strike-slip faults began accommodating displacement along the transform plate boundary [*Frohlich et al.*, 1997; *Lamarche et al.*, 1997; *Massell et al.*, 2000]. Since ~6 Ma, the southeasternmost part of the Australian plate has formed a microplate (the Macquarie plate) that has interacted independently with Pacific crust south of approximately 52° (S. C. Cande and J. M. Stock, Pacific-Antarctic-Australia motion and the formation of the Macquarie plate, submitted to *Geophysical Journal International*, 2003) (hereinafter referred to as Cande and Stock, submitted manuscript, 2003). Subsequent transpression across the Australian-Pacific transform plate boundary has led to uplift along the MRC.

[6] The Australian-Pacific plate boundary between New Zealand's South Island and the Australian-Pacific-Antarctic triple junction varies considerably in orientation, morphology and structure. From north to south, it comprises a continental transform that dissects the South Island of New Zealand (Alpine Fault), a subduction zone at the southern tip of New Zealand with the Australian plate thrusting beneath the Pacific plate (Puysegur trench), an oceanic transform south of New Zealand (MRC), and a zone where subduction is possibly initiating (Hjort trench) (T. A. Meckel et al., Underthrusting at the Hjort Trench, Australian-Pacific plate boundary: Incipient subduction?, submitted to *Geochemistry, Geophysics, Geosystems*, 2003) (hereinafter referred to as Meckel et al., submitted manuscript, 2003) with thrusting of the Australian plate beneath the Pacific plate. The MRC is a ridge and trough system that may be divided southward from New Zealand into four geographic segments: the Puysegur (~330 km long), McDougall (~410 km), Macquarie (~350 km) and Hjort (~300 km) regions [*Hayes and Talwani*, 1972; *Massell et al.*, 2000]. The only subaerial exposure of the MRC is along the Macquarie segment where Macquarie Island and small islets ~11 km north and ~37 km south of Macquarie Island protrude (at a maximum elevation of 433 m) above sea level (Figure 2a). The main active oceanic transform plate boundary fault zone
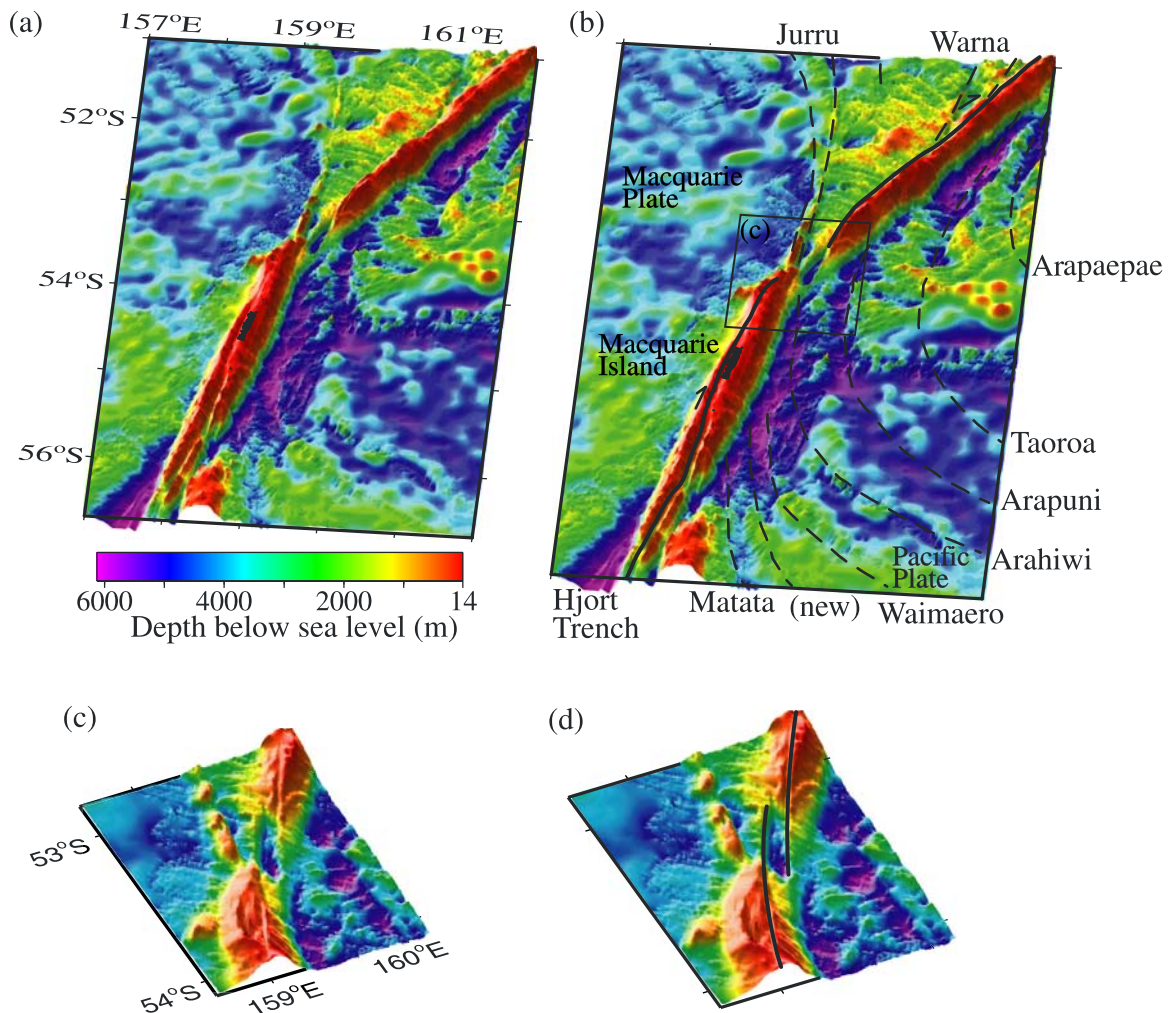
Figure 2. (a) 3D perspective view of the MRC showing the McDougall segment in the north (above ~53°20′S), the Macquarie segment in the south (between ~53°20′S and ~56°40′S) with the northern tip of the Hjort segment in the base of the diagram [after *Bernardel and Symonds*, 2001]. Macquarie Island is at the apex of the Macquarie segment and is shown in black. Mercator projection viewed from 175° at an elevation of 40°. (b) Figure 2a overlain with regional tectonic features. Thick black line is the main Australian-Pacific plate boundary and dashed black lines are fracture zones (from *Massell et al.* [2000] with one new fracture zone identified by magnetic anomaly picks from *Keller et al.* [2002]). (c) 3D perspective view of the transition between the McDougall and Macquarie segments of the MRC. Mercator projection viewed from 200° at an elevation of 40°. (d) Interpretation of an en echelon right step-over in the Australian-Pacific plate boundary. Note the bathymetric low in the pull-apart basin located between the right step-over.

(Figure 2b) is located within a valley between paired ridge crests along the MRC [*Massell et al.*, 2000]. Ridges are not continuous along the MRC. At the transition between the McDougall and Macquarie segments, where the plate boundary has the largest change in strike (~18°), it steps right and coincides with a pull-apart basin ≥5 km deep [*Massell et al.*, 2000] (Figures 2c and 2d). The offset of conjugate fracture zones across the MRC combined with relative poles of Australian-Pacific rotation provide

an estimate of the total brittle displacement across the plate boundary since spreading ceased at ~10 Ma of ~230–290 km [*Keller et al.*, 2002; Cande and Stock, submitted manuscript, 2003].

3. Marine Geophysical Data Analysis

[7] To better constrain the location of the plate boundary and to examine its geometry in detail, we analyzed reflectivity data at 1:500,000 scale
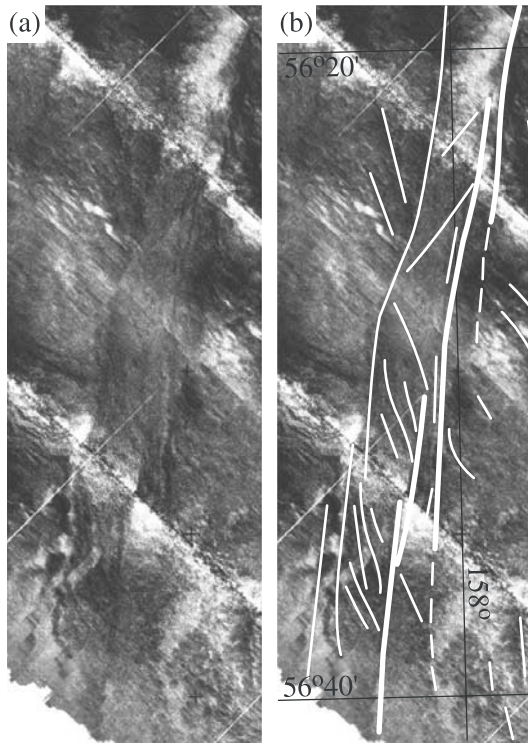
Figure 3. (a) Reflectivity data for the southern end of the Macquarie segment. (b) Interpretation of Figure 3a. Thick white lines are the interpreted active plate boundary and thin white lines are accessory lineaments.

for the McDougall and Macquarie segments of the MRC. A typical reflectivity image from the MRC (Figure 3) shows a 5–15 km wide plate boundary zone for which reflectivity differs markedly from the typical texture of constructional volcanic seafloor (with faulted abyssal hills) outside of the zone. Linear features within the zone approximately parallel the plate boundary and strike at a high angle to the spreading fabric (faulted abyssal hills) on either side of the zone (Figure 3). We follow *Massell et al.* [2000] and define this deformed zone as the Australian-Pacific transform plate boundary fault zone and infer that the lineaments represent active fault scarps.

[8] We have identified 11 main locations along the McDougall and Macquarie segments (Figure 4) where the dominant plate boundary fault displays an en echelon, right step-over geometry (black arrows in Figure 4 and summarized in Figure 5a). The plate boundary fault segments range in length from ~25 km to ~140 km. The width of each step-

over that link plate boundary faults varies from ~1 km to ≤10 km. More lineaments at the right step-over locations are consistent with a higher density of faulting in these locally complex areas. The associated zone of deformation is <5 km wide along the McDougall ridge crest and 5–15 km wide along the Macquarie ridge crest.

[9] Analysis of reflectivity data along ~310 km of the McDougall ridge crest between 51° (Figure 4a) and 53°20′S (Figure 4b) reveals five main fault segments (40–140 km long) offset in a right stepping en echelon pattern. Each long, continuous fault has a narrow zone of associated deformation. Spreading fabric (faulted abyssal hills) may be traced up the flanks of the ridge nearly to the ridge crest. Although the McDougall segment defines a broad arc with the overall strike of the segment changing by 3–4° between the northern and southern ends, faults maintain a similar orientation and vary in strike from 027° to 032°. Four en echelon right steps link the five faults. At these locations, the associated zone of deformation widens and we observe additional N- to NE- trending lineaments. Small bathymetric depressions (2–3.5 km wide and 300–500 m deep), elongate along the plate boundary, coincide with the step-overs and appear to form small pull-apart basins on the ridge. Smaller depressions, typically <100 to 1000 m wide and <100 to 250 m deep, characterize the five main fault segments.

[10] At the transition between the McDougall and Macquarie segments of the plate boundary (Figures 2d and 4b), the average strike of the plate boundary changes by ~18° over a relatively short distance (Figure 4b). Analysis of bathymetric and reflectivity data indicates that this change is accommodated by a ~10 km wide right step in the main plate boundary fault trace linked by a large extensional pull-apart basin (>1 km deep and 38 km long, Figure 2c). We also observe a complex array of lineaments in reflectivity data on the Macquarie segment immediately south of the pull-apart basin, and the fault zone reaches its widest dimension of ~15 km at 53°45′S (Figure 4b). The zone of deformation consists of multiple lineaments oriented generally NNE to NE.
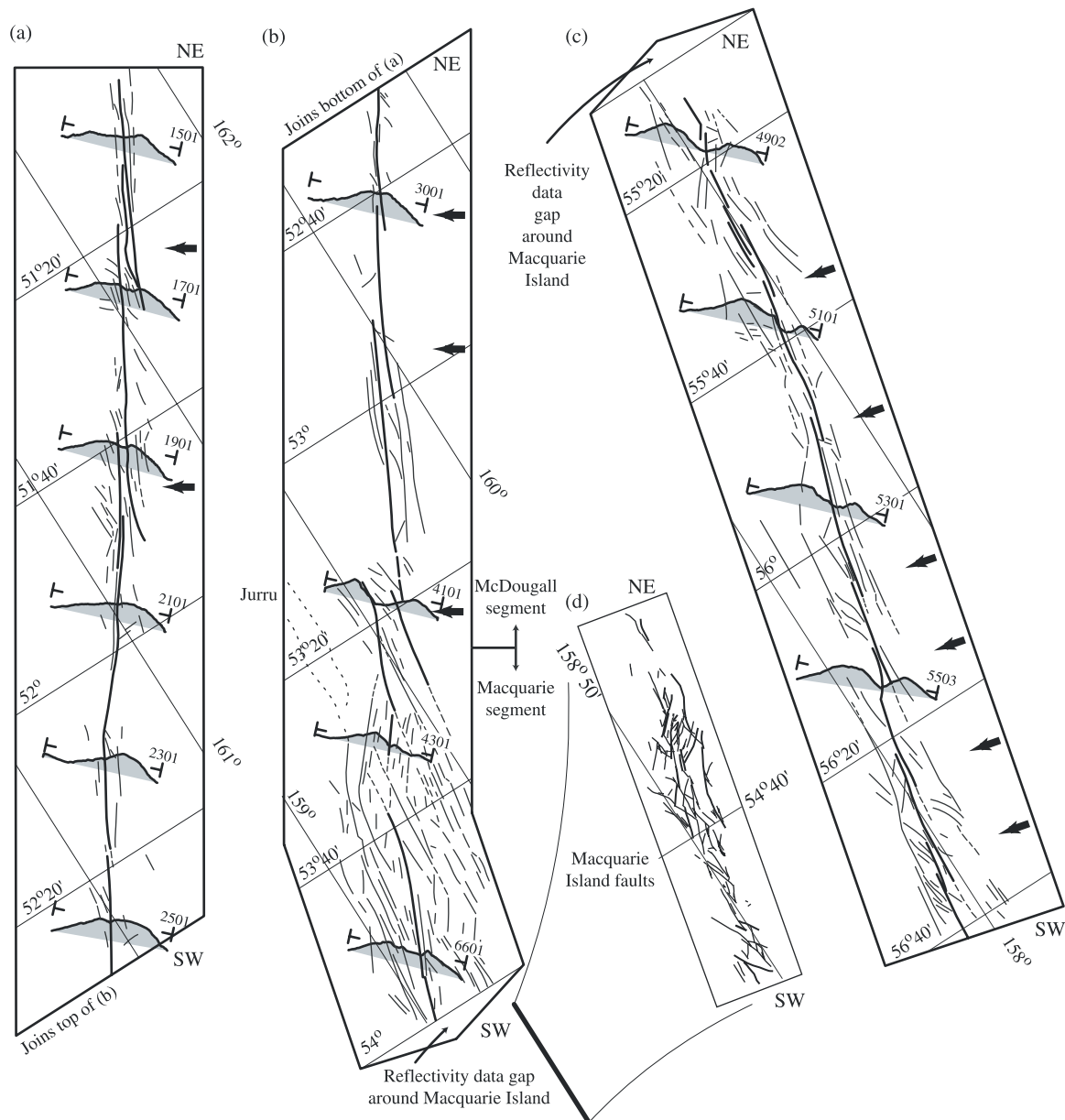
Figure 4. The McDougall and Macquarie segments of the Australian-Pacific plate boundary interpreted from reflectivity data between 51°05′S and 56°40′S. A reflectivity data gap around Macquarie Island between 54°S and 55°10′S is due to shallow water depths and cruise time constraints. Bathymetric profiles (V.E. = 1.75) compiled from interpreted 8-channel seismic reflection data are presented as gray shaded sections (∼21 km long). R/V *Rig Seismic* seismic reflection line numbers are indicated. Thick black line is the interpreted location of the active Australian-Pacific plate boundary. Thin black lines are associated lineaments. Black arrows indicate locations of en echelon right step-overs in the plate boundary. (d) Fault pattern on Macquarie Island observed in data gap. Thick black line at southwestern end of Figure 4b indicates length and general longitude of Macquarie Island data strip. Note northern faults (above ∼54°40′S) are NNE- to NE-striking, similar to those in the seafloor at southwestern end of Figure 4b, whereas those to the southwest are N- to NW-striking similar to seafloor faults in Figure 4c.

[11] Analysis of reflectivity data along ∼170 km of the Macquarie segment south of Macquarie Island between 55°15′S and 56°40′S (Figure 4c) reveals seven shorter, main faults (25–45 km long) in the central valley, linked by six en echelon right steps. Locally, just south of Macquarie Island, the main plate boundary fault consists of short segments (∼10 km long) with both right and left stepping
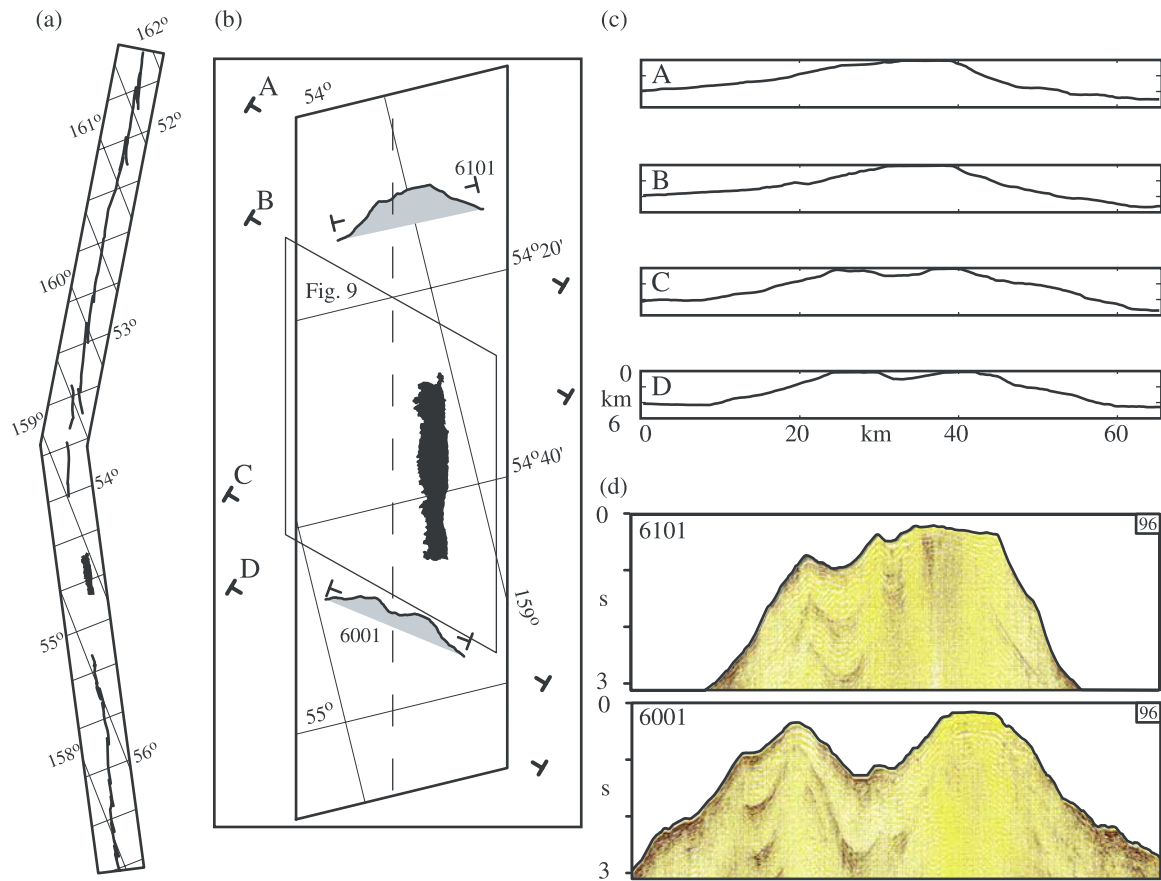
Figure 5. (a) Summary figure compiling the interpreted Australian-Pacific plate boundary from Figures 4a, 4b, and 4c. Note reflectivity data gap around Macquarie Island. (b) Enlargement of the section missing between the bottom of Figure 4b and the top of Figure 4c showing Macquarie Island, bathymetric profiles interpreted from two 96-channel seismic lines and the location of bathymetry profiles shown in Figure 5c (labeled A, B, C and D). (c) Bathymetry profiles (V.E. = 1) drawn from ship track center beam bathymetry data. (d) R/V *Rig Seismic* 96-channel seismic lines 6101 and 6001 showing a single ridge crest north of Macquarie Island and stepped morphology of the central valley just south of Macquarie Island. Note the limited penetration. The profile is ~21 km across and shows depth from 0 to 3 s two-way travel time, or ~0 to 2250 m water depth. The ridge has limited sediment cover and it is difficult to discern any faults into the profile. However, the stepped nature of the seafloor is consistent with active faults controlling the geometry of the profile in the plate boundary zone.

segments. The strike of the dominant faults varies from 010° to 020°, a counter-clockwise change in orientation compared to faults in the McDougall segment. The faults have a similar orientation along the segment length even though the ridge segment is slightly sinuous and southward is continuous with a large curvature along the Hjort segment. The zone of associated deformation is ~8–10 km wide along most of the segment, and NNE-, N- and NNW-trending lineaments also change orientation counter-clockwise relative to those on the McDougall segment. The higher density of en echelon steps has produced an ~200 km long bathymetric depression on top of

the ridge, that widens and deepens toward the south. The valley is ~6–7 km wide and ~1 km deep just south of Macquarie Island, expanding to ~10 km wide and >1 km deep at the southern end of the Macquarie segment.

[12] To augment the reflectivity data, bathymetric profiles were interpreted from seismic reflection data across the MRC. These profiles reveal variability in ridge morphology associated with the right step-overs (Figure 4): a single ridge crest is associated with long linear segments of the plate boundary distal to step-overs, whereas double ridge crests and central valley depressions correspond to

locations with right step-overs. We interpret the valleys as pull-apart basins associated with right steps in the dextral strike-slip plate boundary as discussed further below.

[13] Bathymetric profiles across the pull-apart basin at the transition between the McDougall and Macquarie segments of the plate boundary (Figures 2 and 4) and the lineaments in the reflectivity data (Figure 4b) indicate that the pull-apart basin is ~38 km long by 10 km wide. The deepest part of the pull-apart basin is ~5.2 km below sea level and is located at the SE corner of the basin floor (Figures 2c and 2d). The average relief between the basin floor and the top of the ridges that bound it is ~1.2 km. Ridges at the southern end of the McDougall segment and the northern end of the Macquarie segment have similar morphology; both reach within 1 km of sea level, are 25–30 km wide at their bases and contain minor trenches on their eastern sides.

[14] Bathymetric profiles across the northernmost part of the Macquarie segment indicate a number of small depressions and ridges across the ridge crest, consistent with a broad zone of currently active faults. For the rest of the northern Macquarie segment, only limited reflectivity, seismic reflection and bathymetric data are available around Macquarie Island because of shallow water depths and cruise time constraints. To better understand the nature of the plate boundary in the vicinity of Macquarie Island, we have examined the available seismic reflection profiles (Figures 5b and 5d) and four bathymetric profiles (compiled from center beam ship track bathymetry data; Figure 5c) north and south of the island. A single crest characterizes the ridge immediately north of the island, in contrast to a double crest immediately south of the island (Figures 5b and 5c), indicating that the island lies within the transition region between a single fault strand and a step-over. In addition, the general fault orientation changes from NNE- and NE-trending lineaments north of the island to NNE-, N- and NNW-trending lineaments south of the island (Figure 4).

[15] Bathymetric profiles also show the anomalous topography of the MRC. North of the island,

the ~10 km wide, flat-topped, single ridge crest is only ~50 m deep, consistent with previous exposure of large tracts of the Macquarie segment to marine wave action. The steepest ridge slope (eastern flank) in the vicinity of the island is ~30° (Figure 5c, Profile A). Most other flanks of the McDougall and Macquarie ridges dip at ~15°. North of Macquarie Island, the ridge is ~50 km across at its base and is flanked by a trough to the east. At Macquarie Island and to the south along the Macquarie segment, the ridge is double crested (Figures 2a and 5c). Macquarie Island is located on the eastern crest. South of the island, the flat-topped, ~70 m deep double crests are well developed (Figure 5c, Profiles C and D). Each ridge crest is ~4–6 km across, and the central valley between them is ~7 km across and ~900 m deep. South of Macquarie Island, the ridge is ~50 km across at its base, and the MRC has the largest cross-sectional area here. The trough on the E side of the ridge is ~5.5 km deep (Figure 5c, Profile C).

[16] Although the central valley of this southern portion of the Macquarie segment is morphologically similar in cross section to the pull-apart basin located at the boundary between the McDougall and Macquarie segments, it is over 200 km long (Figure 2a) and extends south of the study area for at least another 200 km as the plate boundary curves dramatically in the contiguous Hjort segment. We observe no large step (~10 km) in any of the faults inferred from reflectivity data to account for the large valley along much of the Macquarie segment (Figures 4c and 5). The valley may be controlled by the numerous faults across the valley floor, more of which may lie buried beneath mass wasting debris and other sediment. We infer that the high density of small step-overs in these valley faults controls the continuous nature of the valley as discussed later.

4. Macquarie Island

[17] Macquarie Island is located ~4.5 km east of the active Australian-Pacific transform plate boundary (Figure 5). Reflectivity data shows that the transform comprises a ~15 km wide zone of

closely spaced NNE- to NE-trending lineaments north of the island and a ∼8–10 km wide zone of NNE to NNW-trending lineaments south of the island (Figure 4). Therefore it is most likely that Macquarie Island is located within these lineament zones and exposes features similar to those mapped from reflectivity data. Thus these exposures allow us to test our interpretations of the geophysical data and to examine the type, geometry, and interrelationships of the faults in this critical area.

4.1. Field Data

[18] Macquarie Island comprises fault-bounded blocks made up of all levels of oceanic crust and upper mantle from extrusive lavas and minor sedimentary rocks to sheeted diabase dykes, gabbros, and serpentinized peridotites (Figure 6a) [*Varne et al.*, 1969, 2000; *Varne and Rubenach*, 1972; *Christodoulou et al.*, 1984; *Goscombe and Everard*, 1998]. Recent faults dissect the entire island but are dominant in the volcanic rocks of the center third of the island, creating long, linear ridges and basins (Figure 6, profiles C–G). The ultramafic and plutonic rocks of the northern end have a smoother, less rugged topography with broad, flat-topped mountains (Figures 6b and 6c, profile K). The volcanic rocks of the southern end have formed many sharp craggy peaks with some linear fault scarps (Figures 6b and 6c, profile K).

[19] We examined the most prominent of the ∼150 recent faults and fault scarps identified and mapped by *Goscombe and Everard* [1998, 2001], excluding faults of limited extent or lacking clear topographic expression or exposure. We measured strike, length, and throw, as well as noting the location, rock types cut and cross-cutting relationships of faults and other prominent features (Table 1). Overall, recent faults on the island exhibit almost exclusively normal and oblique normal motion. The topography of the central portion of the island is dominated by en echelon NE and NNE faults that step to the right and left, forming pull-apart basins or relay faults that link the larger faults. In many cases, faults die out and motion is relayed to a nearby parallel fault. Southward, the primary fault strikes change to NNW and NW. These NW faults truncate the NE ones and are less distinct, but

display similar en echelon relationships and normal-oblique motion.

[20] Throughout the island, faults with scarps are linear to curvilinear and extend for hundreds of meters up to ∼7 km along strike. Most, however, extend continuously for 500 m to 1 km along strike and terminate at intersections with other recent fault scarps, or their scarps gradually diminish along strike over a distance of a few tens to hundreds of meters. Most recent fault scarps have throws of 5–15 m, but the larger scarps are up to 150 m high. These measurements provide a minimum estimate for total vertical movement, however, as marine wave action would most likely have removed any topography produced on these faults prior to emergence of the island above sea level.

[21] The strike of recent faults (Figure 7a) ranges from WNW to NE (Figure 7a). We have weighted these data for length along strike (Figure 7b) and for throw (Figure 7c). The NNE- to NE-striking recent faults are by far the most laterally continuous and also show the largest throw, and therefore provide the most significant constraints on the tectonic models as discussed further below. Additionally, the major recent faults change in strike along the length of the island from generally NE- and NNE-striking in the north to N-, NW- and NNW-striking in the south (Figures 6b and 6c); this corresponds to the pattern observed in the marine geophysical data, indicating that the island records the transition between the patterns of fault orientations north and south of the island (Figure 4).

[22] Most major recent faults on the island show a dominantly normal sense of motion (Table 1). Horsts and grabens are common, and normal displacement is transferred across en echelon faults on relay ramps. Accurate kinematic analysis of these faults is difficult, however, given limited exposure of actual fault planes; most fault planes are eroded or buried by mass wasting debris. Topographic relief clearly constrains estimates of vertical movement. We observed only limited strike-slip displacement on outcrop-scale faults; the similarity of geologic units across major faults precluded using offset of units or marker horizons to determine lateral displacements. *Goscombe and Everard*
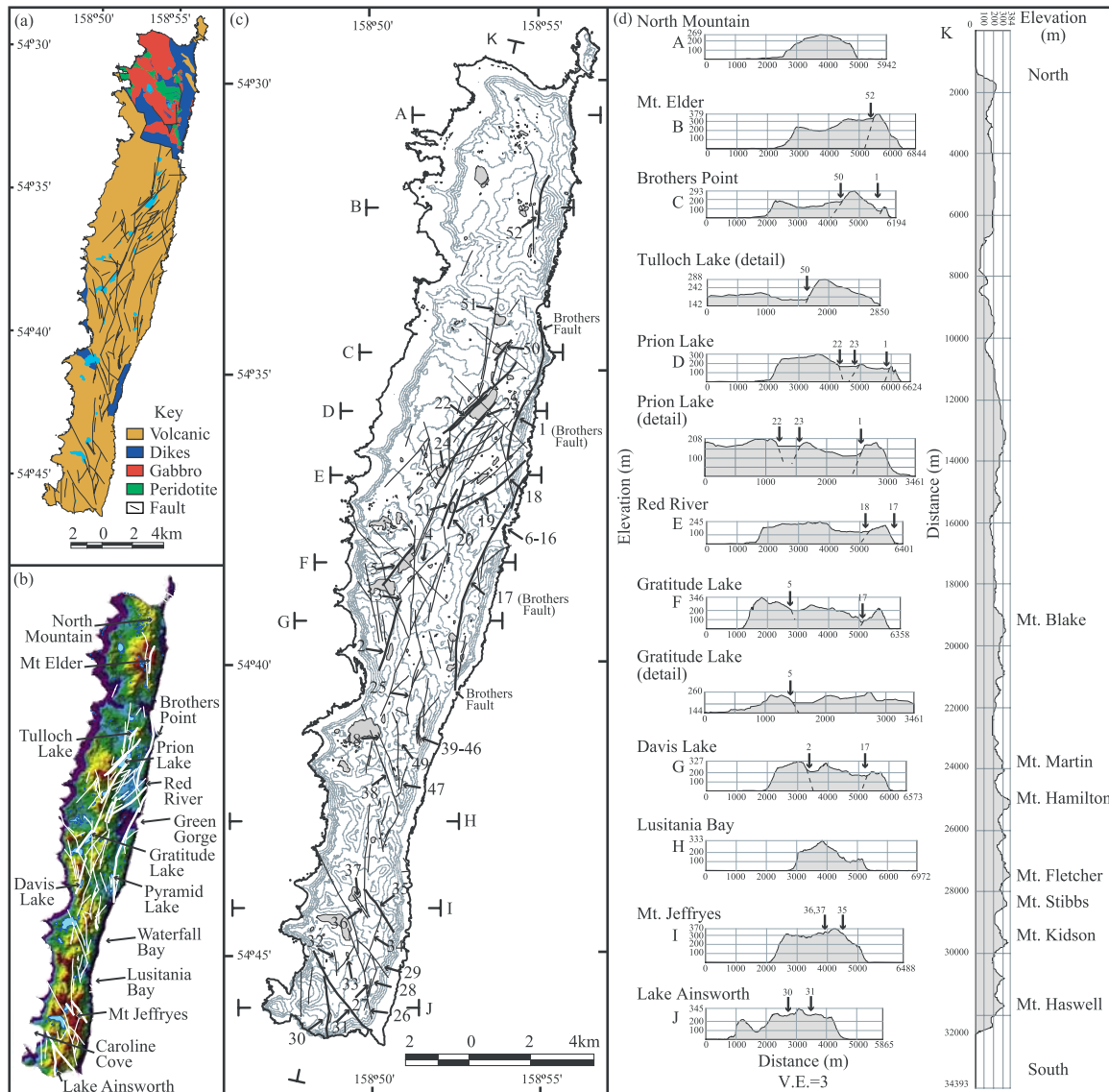
Figure 6. Field data from Macquarie Island. (a) Geologic map of Macquarie Island [after *Goscombe and Everard*, 1998]. The island has a complete suite of oceanic rocks, from upper mantle to upper crustal rocks. Map shows both the recent faults examined in this study, as well as faults that formed during seafloor spreading. (b) Shaded relief topography image of Macquarie Island. The Brothers fault and related faults create linear valleys along the central- and north-eastern coast. Other faults form pull-apart basins that contain lakes. Geographic locations mentioned in the text are labeled. (c) Recent faults on Macquarie Island superposed on topographic contours. Bold lines are major faults with significant fault scarps; other lines are smaller recent faults. Numbered faults correspond to those in Table 1. T-bars mark cross section lines in Figure 6d. Three shorter cross sections (detail profiles in Figure 6d) are marked with lines. (d) Topographic profiles of Macquarie Island. The steep sides of the island are not cliffs generated by faults; they form via mass wasting as the island is uplifted with the ridge complex. Numbered faults correspond to Figure 6c and Table 1. Faults with obvious scarps have been projected with dashed lines. Note that lake depths are unknown at present and flat areas in the profiles with lakes represent water level at time of survey. Profile K shows the topographic change from north to south, from rounded mountains in the north to rocky peaks dominating the south.

[2001] estimate lateral displacements ranging from 80 to 2500 m; however, the only two large displacements (1 km and 2.5 km) are based on apparent offset of seafloor spreading-related faults. Our

fieldwork has demonstrated that these spreading-related faults formed with this stepped geometry [*Wertz et al.*, 2003]; thus these large lateral displacements are not the result of recent strike-slip faulting.

Table 1. Recent Fault Data[a]

Fault	Length, m	Strike	Upthrown Block	Throw, m	Rock Unit	Location	Comment
1	4300	030	120	100	P-D	BP	Brothers fault at Brothers Point
2	2400	200	290	10	P	DPP	Davis lake
3	300	166	256	0	P	DPP	Offsets Davis lake fault (2 and 4)
4	2000	225	315		P	DPP	Continuation of Davis lake fault
5	1600	220	310	8	P	GL	Gratitude lake
6	20	105	195		P	GG	Brothers fault graben 1
7	20	110	200	2	P	GG	Brothers fault graben 2
8	20	290	020	10	P	GG	Brothers fault graben 2
9	20	110	200	10	P	GG	Brothers fault graben 3
10	20	290	020	6	P	GG	Brothers fault graben 3
11	25	120	210	6	P	GG	Brothers fault graben 4a
12	25	300	030		P	GG	Brothers fault graben 4a
13	5	100	190	6	P	GG	Brothers fault graben 4b
14	5	280	010		P	GG	Brothers fault graben 4b
15	20	110	200	2	P	GG	Brothers fault graben 5
16		090	180		P	GG	Brothers fault graben 6
17	7400	018	108	150	P	GG	Brothers fault from GG to PL
18	1000	060	150	10	P	GG	N end of fault, switches upthrown midway
19	1000	240	330	10	P	GG	S end of fault, switches upthrown midway
20	1600	025	115	30	P	LI	Lake Ifould fault east bank, wave cut platform
21	1600	205	295		P	LI	Lake Ifould fault, west bank
22	3300	225	315	50	P	PL	Prion NW, height ranges from 5–50 m, from NE-SW
23	1000	035	125		P	PL	Prion SE a
24	2200	045	135	50	P	PL	Prion SE b, varies in throw from 1–50, NE-SW
25	800	045	135	10	P	WBP	Plateau W of WB, near layered picrite along track
26	3000	344	074	5	P	HP	N-most end throw increases to 20m, controls drainage, truncates 27 and 28
27	500	012	102	4	P	HP	Small fault parallel to Brothers system
28	1000	020	110	5	P	HP	East of 27
29	450	342	072	5	P	HP	Truncates 28
30	500	185	275	10	P	LA	Lake Ainsworth fault
31	2000	320	050	10	P	HP	Fault that veers out from SE bay. Dies out to the NW
32	500	313	043	5	P	WL	Little fault S of WL
33	1200	030	120	10	P	WL	Bounds small lake S of WL
34	1200	020	110	20	P	MJ	Mt Jeffryes fault, decreases to 5 m to S
35	1600	325	055	10	P	MJ	Mt Jeffryes, truncates 34
36	800	327	057	5	P	WR	Windy Ridge horst, S
37	800	147	237	5	P	WR	Windy Ridge horst, N
38	600	155	245	10	D-P	ML	Enters major lake, dies quickly
39	400	005	095	5	P	WBP	Westernmost of curved faults
40	190	350	080	5	P	WBP	have split into 2 faults at bend
41	450	345	075	5	P	WBP	2nd from west
42	550	005	095	5	P	WBP	3rd from W, N end
43	230	335	065	5	P	WBP	S end
44	530	005	095	5	P	WBP	Easternmost fault, N
45	230	335	065	2	P	WBP	S end
46	410	360	090	10	P	WBP	This and next two are related, hard to follow
47	730	340	070	5	P	WBP	
48	960	355	085	5	P	WBP	
49	900	040	130	50	P	TL	Tulloch Lake
50	3000	008	278	20	P	SL	Square Lake
51	1300	010	100	40	M	ME	Mt Elder

[a]Rock units: P, pillow basalt; D, sheeted dykes; M, peridotite. Locations: BP, Brothers Point; DPP, Davis Point Plateau; GL, Gratitude Lake; GG, Green Gorge; LI, Lake Ifould; PL, Prion Lake; WBP, Waterfall Bay Plateau; HP, Hurd Point; LA, Lake Ainsworth; WL, Waterfall Lake; MJ, Mt. Jeffryes; WR, Windy Ridge; ML, Major Lake; TL, Tulloch Lake; SL, Square Lake; ME, Mt. Elder. All fault locations are numbered in Figure 6.
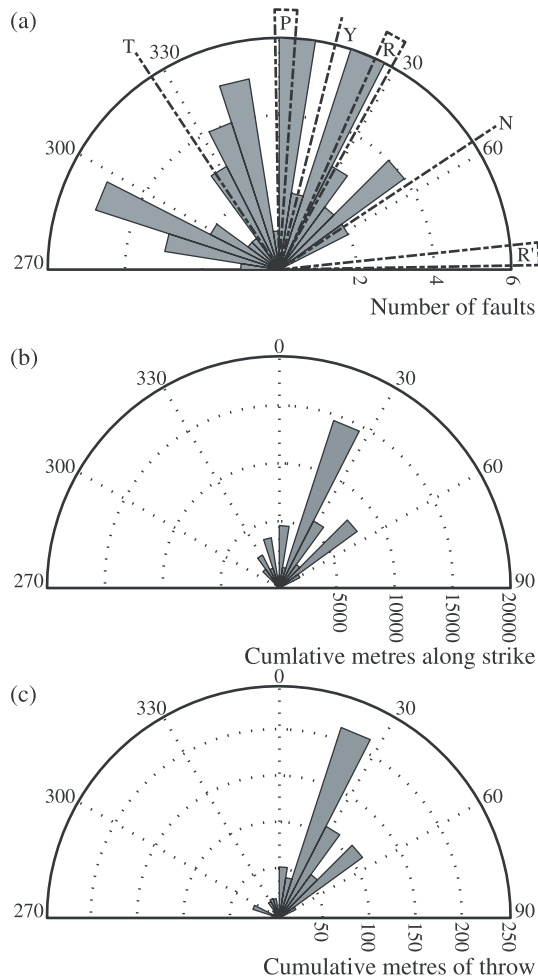
Figure 7. (a) Rose diagram of the strike of recent fault data shown in Table 1. The orientations of the plate boundary (Y) and expected secondary faults for classical wrenching (R, R'-Riedel and P-primary shears; N-normal, T-thrust faults) are overlayed. The data do not fit the predicted fault orientations and types. (b) Data shown in Figure 7a weighted for along strike length of the faults showing that the longest recent faults are within the NNE-striking group. (c) Data shown in Figure 7a weighted for throw showing that the faults with the largest throw are within the NNE-striking group.

Unlike *Goscombe and Everard* [2001], we found no evidence for transpression. The thrust faults they mapped in the northern end of the island show no topographic relief. We reinterpret their faults that place volcanic rocks on dolerite dykes as depositional contacts, an interpretation similar to that of other workers [*Alt et al.*, 2003]. Faulting and fracturing in this area occurs beneath the actual

contact. Their other thrust fault that places ultra-mafic rocks on dykes was too poorly exposed as a result of mass wasting for us to verify it.

[23] We now discuss the recent faults that occur on Macquarie Island from north to south.

4.1.1. Northern Recent Faults

[24] We observe few recent faults in the northern third of the island, possibly due to the style of erosion of the plutonic and serpentinized ultramafic rocks. Near Mt. Elder (Figures 6b and 6d, profile B), NNE- to NE-striking faults show 5–20 m high scarps, but they are less continuous than those in the central region of the island.

4.1.2. Central Recent Faults

[25] The Brothers fault is the most extensive recent fault on the island, located along the central east coast (Figures 6c and 8a; Table 1). From Brothers Point to Waterfall Bay (Figure 6b), the fault has created a steep scarp of varying heights. At Brothers Point, the fault shows slickensides and striations with a >80° pitch down dip to the south on moderately (~50°) W-dipping fault planes (Figure 8b). The topographic offset (W-side down, Figure 8a) and small steps on fault planes indicate a normal sense of motion (Figure 8b). Normal dip-slip lineations surround the southern end of the Alpine Fault segment of the Australian-Pacific plate boundary within 1–100 m of the principal displacement zone, which is also dominantly strike-slip [*Sutherland and Norris*, 1995]. The Brothers fault becomes less defined in two locations, near Red River (Figures 6b and 8c) and Green Gorge (Figures 6b and 8d), where displacement is transferred to other fault segments (Figure 6). These transfer zones contain minor, less continuous, faults oblique to the Brothers fault, which have less prominent scarps (Figures 8c and 8d). In the Red River area, the fault scarp tapers off southward and then picks up displacement on another major segment farther to the east (Figure 8c). The intervening transfer zone contains NNE- to NE-striking faults, and the faults are less distinct, lacking the sharp scarps of the Brothers fault. The NE-striking faults appear to act as links between the two major traces of the Brothers fault.
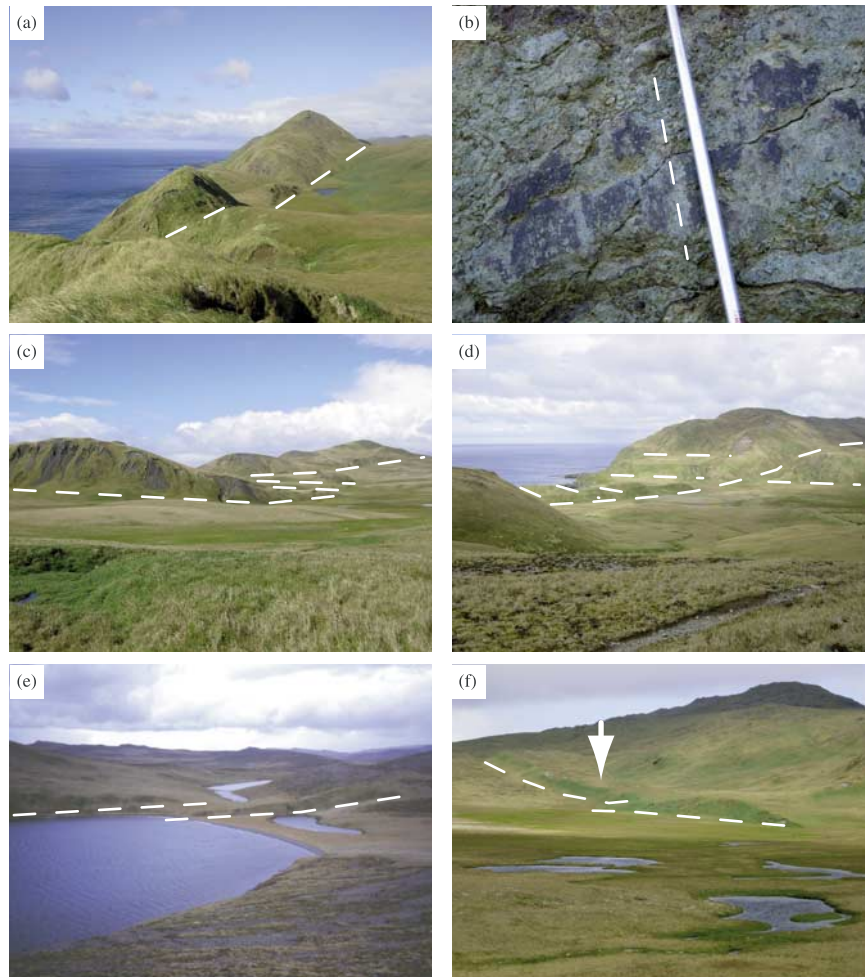
Figure 8. (a) The Brothers fault scarp, looking south (fault 1, Figure 6, Table 1). The maximum estimated height of the scarp at this location is ∼150 m. White dashed lines indicate the base of the W-dipping scarp. (b) Exposure of the Brothers fault. Dashed white line shows orientation of down-dip slickensides. Ski pole is ∼1−1.5cm across. (c) The Brothers fault transfer zone at Red River (Figure 6), looking SE. White dashed lines mark fault traces in the transfer zone. The maximum estimated height of the scarp at this location is ∼50 m. (d) Green Gorge catchment, looking SE. White dashed line running parallel to the coast marks the Brothers fault. White dashed lines running at a high angle to the coast are graben-bounding faults (faults 6−16, Figure 6, Table 1). The maximum height of the scarps at this location is ∼20 m. (e) Northern end of Prion Lake, looking NNW (fault 22, Figure 6, Table 1). The white dashed line marks the fault that bounds the NW-shore. This fault steps to the right at the NE end of the lake. The maximum estimated height of the scarp in view is ∼15 m. (f) Horst west of Red River, looking SW. White dashed lines mark the base of the foreground fault scarp of the horst pair. The white arrow marks the top of the background fault scarp. The maximum estimated height of the foreground scarp at this location is ∼5 m.

One of the NE-striking faults changes the up-thrown side halfway along its length, with the northwest side up at the southern end, and the southeast side up at the northern end, apparently caused by a counter-clockwise rotation. Also in this area, two NNW-striking faults affect the topography, but the NE-striking faults are dominant. In the Green Gorge area, where the fault steps slightly to the right (Figure 6c), a series of small grabens and half

grabens (∼20 m long and 5−41 m wide, bounding fault scarps 2−6 m tall) with NW strikes are within the transfer zone (Figure 8d). The Brothers fault cuts the northern set of grabens, suggesting that the fault propagated north into the pull-apart basin after the grabens formed.

[26] In the central section of the island, en echelon faults form pull-apart basins or half-graben lakes

(e.g., Prion Lake, Gratitude Lake, Figure 6, profiles D and F). These basins all trend NNE to NE and are generally asymmetric with one dominant bounding fault. Prion Lake is the largest example (Figure 6, profile F and Figure 8e). The scarps that form this lake range from 5–50 m in height, with the NW scarp more pronounced. The pull-apart basin is formed by a left step, from the fault that forms the SE side of the lake to the fault that forms the NW side (Figures 6b and 6c). At the northern end of the lake, the primary northwest fault tapers off, and the motion is picked up by a parallel fault a few meters to the east, which forms a linear scarp for ~20 m (Figure 8e). This type of relay between en echelon faults is common across the island. En echelon faults also form horsts in this part of the island (Figure 8f).

4.1.3. Southern Recent Faults

[27] South of Pyramid Lake (Figure 6b), the Brothers fault and other NE faults have less definition, and we observe more NNW and NW faults. Although NNE and NE faults dissect the southern region, they are frequently truncated (e.g., Mt. Jeffryes; Figure 6c between profile I and J) or offset (Mt. Blake; Figure 6c, fault 3) by the NNW and NW faults. No faults in this region are as continuous as the Brothers fault to the north, and faults frequently die out along strike. A well-developed horst and poorly developed graben pair (327° strike, Figure 6c, faults 35–37) is found near Mt. Jeffryes. Only one half-graben lake is observed in the southern end of the island (Lake Ainsworth, Figure 6b); its scarp can be followed for 500 m.

4.2. Petrologic Data

[28] We identify three types of recent faults on the basis of petrology: the most common "Brothers-type" after the Brothers fault, "spaced discrete-type" faults, and "clay and mica cataclasite-type" faults.

4.2.1. Brothers-Type Faults

[29] Zones of deformation associated with individual Brothers-type faults are most commonly less than 50 mm wide and consist of cohesive breccia that is weakly foliated in hand sample. Well-devel-

oped slickensides and striations exist on discrete fault planes. The best example is located in the creek gully NW of and adjacent to the Brothers Point field hut where a recent slump on the gully flanks has exposed the Brothers fault (GR494650E, 3952550N). This fault type is by far the most common and encompasses most recent faults with fault scarps. Wall rock fragments within the breccia are generally less than 1 mm across but may be up to 70 mm. The fragments are sub-rounded to angular with the larger fragments faceted, but rounded. The fragments include (i) wall rock basalt or diabase depending on what lithology is deformed, and (ii) single mineral fractions of constituent grains within the wall rock such as albite, diopside and tremolite. Where these recent faults cut older faults related to seafloor spreading, quartz, epidote and minor sulphide may be found as fragments by themselves or as minerals within fragments of wall rock related to hydrothermal mineralization in the older fault. The fine-grained matrix mostly comprises fine-grained wall rock fragments.

4.2.2. Spaced Discrete-Type Faults

[30] Zones of deformation associated with individual spaced discrete-type faults are less than a few mm wide; these discrete faults form in zones 20–25 m wide with faults spaced ~2–6 m. This type of fault is generally uncommon and the best example is located ~500 m north of the Green Gorge field hut in coastal wave-cut exposures (GR493840E, 3946760N). At this locality, individual, discrete, steeply-dipping faults cut hyaloclastite and offset narrow dykes with normal motion and throw of <1 to ~10 m, indicating that the cumulative throw on the zone of spaced discrete faults may be up to ~40 m. We observe minor alteration zones (~20 mm wide) in hand sample adjacent to the discrete faults. No slickensides or mineralization are evident on the fault surfaces. In the Green Gorge example, the clasts in the hyaloclastite are most commonly glass and rarely basalt and single grains of plagioclase; rims of the glass clasts are altered at their margins and also along vesicle rims. The alteration is most intense closest to a discrete fault plane where calcite fills some vesicles. The wall rock is

undeformed, suggesting that strain was partitioned only into the discrete faults.

4.2.3. Clay and Mica Cataclasite-Type Faults

[31] The clay and mica cataclasite-type fault zones are most commonly a few centimeters wide and consist of moderately friable cohesive cataclasite that may or may not be foliated in hand sample. This type of fault is also generally uncommon or poorly exposed. Samples dominated by chlorite show well-developed down-dip slickensides and striations (e.g., plunging 65° toward 078°) on slaty cleavage planes (e.g., 167/64/E), whereas samples dominated by mixed clay and muscovite are weakly foliated. The best examples of the clay and mica cataclasite-type fault zones are located adjacent to the walking track, in the creek less than 100 m upstream from the old Caroline Cove (Figure 6b) field hut site (GR496610E, 3931450N). Wall rock fragments within chlorite dominated cataclasite show a broad range in sizes; most fragments are commonly less than 1 mm across but may be up to 3 mm. The fragments are sub-rounded to angular with the larger fragments displaying the most rounded shapes. The fragments include (i) polycrystalline fine-grained basalt, and (ii) mono- or polymineralic fractions of quartz, epidote, and/or sulphide. The presence of quartz, epidote and sulphide strongly suggests that the fragments are most likely partially derived from a preexisting fault related to seafloor spreading. Thin ($\ll$1 mm) quartz and/or epidote veins that cut some basalt wall rock fragments, but are restricted to the fragment, are consistent with this interpretation. Furthermore, quartz fragments are generally single crystals, but some polycrystalline quartz fragments contain irregular to straight grain boundaries consistent with grain boundary migration recrystallization. Only the seafloor-spreading phase of deformation evolved at temperatures high enough to allow dynamic recrystallization of quartz. The fine-grained matrix mostly comprises very fine-grained wall rock fragments and chlorite. In the clay-rich samples, muscovite and an $\sim$70% illite/30% smectite mixed-layered clay (identified by powdered X-ray diffraction analysis) are randomly oriented in the section. Fragments of wall rock are rare and very small ($\ll$1 mm across). The growth of new minerals in the clay and mica cataclasite-type faults suggests that they evolved at higher temperatures and with higher fluid flow than the more common Brothers-type dry breccia faults. As the clay and mica cataclasite-type faults do not show active scarps, we suggest that these most likely evolved prior to emergence of the island above sea level.

[32] In summary, recent faults on Macquarie Island are commonly cohesive breccia zones with throw across the fault of $\sim$5–15 m. However, we interpret an earlier phase of clay and mica cataclasite-type faults that likely evolved in the submarine environment when hydrothermal fluids were moving through the faults, aiding growth of new clay and mica minerals. These faults were only identified in the creek that drains into Caroline Cove and we suggest that the clay and mica cataclasite-type faults probably exist in other parts of the island but are rarely exposed due to their friable nature. As we only noted spaced discrete-type faults in close proximity to the Brothers fault itself, we also suggest that the discrete-type faults are genetically related to large Brothers-type faults.

5. Discussion

5.1. Comparison of Island and Marine Geophysical Data

[33] Macquarie Island lies within the zone of deformation at the currently active plate boundary. The patterns of faulting on the island and of the lineaments mapped on the seafloor within the ridge crests using reflectivity data (Figure 4) are equivalent, thus validating our interpretation of these lineaments as recent faults. Faults on the island occur as a series of en echelon faults that step to the right and left, forming pull-apart basins and relay zones (Figure 6). Numerous, differently oriented, smaller faults occur in these transfer zones, accommodating strain where displacement is transferred from one fault segment to another. Although on a different scale, these relationships match our interpretation of the plate boundary fault zone using marine geophysical data. The presence of these finer scale features on Macquarie Island indicates
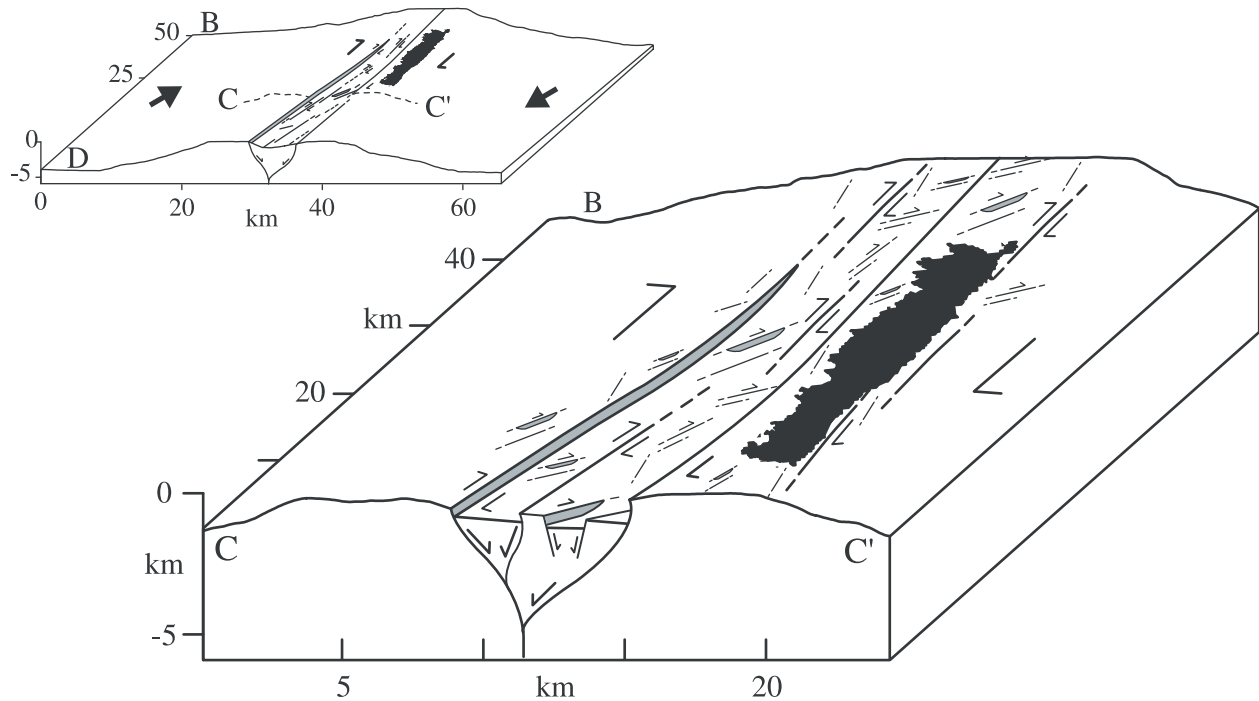
Figure 9. Block diagram model of the faulting patterns on the Macquarie segment of the MRC near Macquarie Island. Profiles B and D from Figures 5b and 5c form the northern and southern ends of the block diagram (V.E. = 1). Profile C-C' is the central part of profile C in Figure 5c (V.E. = 1). Thick black arrows represent plate motion vectors that are ∼20° oblique to the plate boundary.

that the larger basins within the ridge crests are composed of numerous smaller pull-apart basins and extensional relay zones that help accommodate the overall deformation.

[34] The dominant fault orientation on the island changes from NE-striking with minor NNE- striking faults in the north to NW- and N-striking with minor NNE-striking faults in the south (Figure 6). Although the orientation changes, the faults form a similar en echelon pattern, indicating similar processes formed them. It appears that the NNE-striking faults formed first, and were truncated or offset by later NW-striking faults. This change in orientation records the change in orientation observed between the plate boundary faults and associated lineaments to the north and south of the island (Figure 4).

[35] Most recent faults on the island show primarily normal motion (with a minor component of oblique right lateral motion), in apparent contrast to the island's right lateral transpressional tectonic setting and recent history of uplift. We interpret the recent faults on Macquarie Island as forming in response to local extensional stresses associated with right steps in the Australian-Pacific plate boundary located ∼4.5 km west of the island (Figure 9).

[36] Our petrological analysis of the recent faults on Macquarie Island suggests that the mode of deformation within the faults has most likely changed with time and emergence of the island. The earlier generation of recent faults most likely formed in young oceanic crust with a higher geothermal gradient, when the island was still submerged with remnants of hydrothermal fluid circulation. The most recent generation of faults on Macquarie Island possibly reflect a lower geothermal gradient along the plate boundary and different stress fields at the convergent margin may have inhibited fluid flow.

5.2. Genesis of Secondary Faults

[37] Continental transform plate boundaries commonly show a variety of secondary structures such as Riedel and primary shears (R, R' and P), normal faults, and thrust faults [*Wilcox et al.*, 1973;
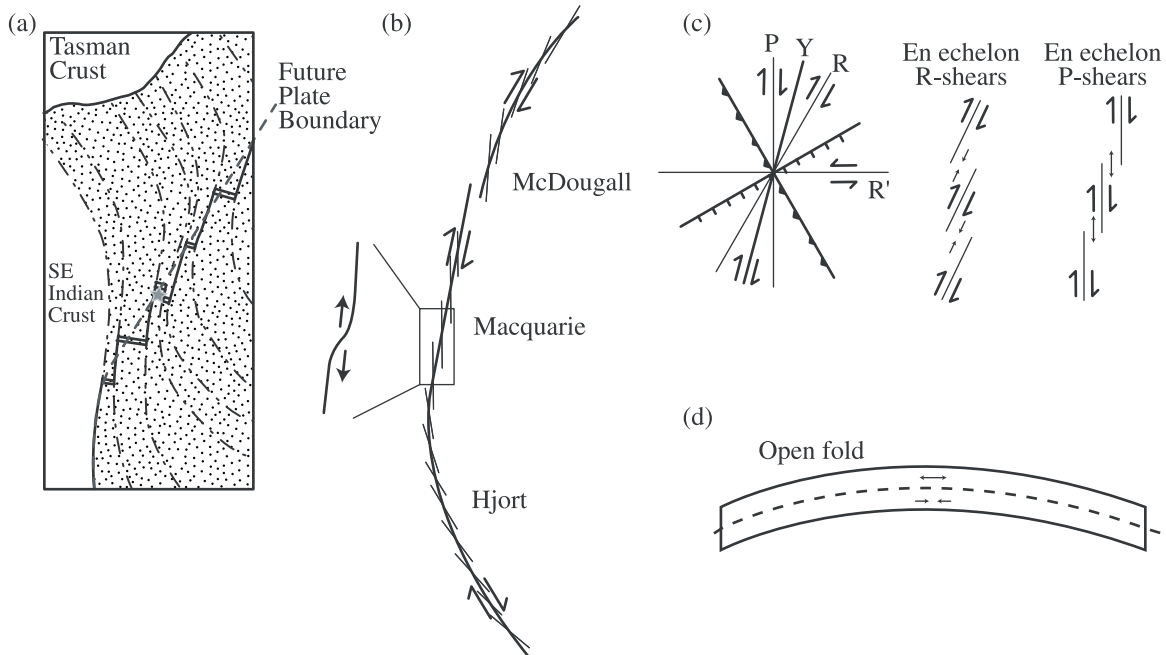
Figure 10. (a) Cartoon interpretation of the plate boundary geometry at ~10 Ma when spreading ceased. Stippled pattern shows crust formed at the Macquarie spreading center between ~40 and ~10 Ma. Small star locates our best estimate of where Macquarie Island formed. (b) Summary diagram showing the overall preexisting curvature to the Australian-Pacific plate boundary and en echelon right lateral plate boundary faults that formed conforming to this geometry. Curvature on the McDougall segment, angle between plate boundary faults and plate boundary, and blow up of the releasing bend geometry along the southern Macquarie segment are exaggerated. (c) Classic wrench model for secondary faults and the two simplest en echelon geometries for right lateral bulk shear. Y-shears parallel the bulk shear. R- and P-shears show synthetic motion (right lateral in our case), R'-shears show antithetic motion (left lateral in our case). (d) A model showing a 50 km wide, 5 km tall open fold. The dashed line locates the neutral surface, above and below which the lithosphere would experience extension and contraction, respectively.

Sylvester and Smith, 1976; *Naylor et al.*, 1986; *Keller et al.*, 1997] in orientations similar to those produced in analogue materials undergoing wrenching [*Naylor et al.*, 1986; *Casas et al.*, 2001] (Figures 7a and 10c). For transpressional settings, field observations and analogue modeling, have shown that the secondary structures change orientation, and which secondary features are dominant changes as well [*Keller et al.*, 1997; *Casas et al.*, 2001] (Figure 7a). *Goscombe and Everard* [2001] proposed that recent faults on Macquarie Island match predicted geometries for secondary faults. Across the island, however, we have found dominantly normal faults, in all orientations, with a minor component of strike-slip motion and no evidence for thrust faulting. Recent fault orientations and those predicted by a right lateral shear couple along a N14°E plate boundary (Figure 7a) do not correspond. Few observed faults are in the correct orientation for normal motion, and most are not in any predicted orientation. N- to NNE-striking faults are predicted to be right lateral strike-slip faults; instead they are dominantly normal faults. Transpression rotates the predicted fault orientations clockwise, which makes any correlation worse.

5.3. Genesis of Plate Boundary Faults

[38] The major faults that comprise the submarine plate boundary fault zone must accommodate significant strike-slip displacement. Offset of conjugate fracture zones across the MRC indicates ~230–290 km of right lateral displacement since spreading ceased at ~10 Ma (Figure 1) [*Keller et al.*, 2002]. The en echelon faults generally subparallel the overall plate boundary strike, and the associated zone of deformation is analogous to the ~1 km wide "Transform Fault Zone" recognized at ridge-ridge transforms such as the Clipperton transform [*Gallo et al.*, 1986; *Kastens et al.*, 1986].

[39] En echelon faults, similar to those comprising the plate boundary faults, are observed in transpressional regimes. For minor transpression, analogue (sand and clay box) models of strike-slip faults show either R- or P-shears dominating. When R-shears dominate, the stepping direction between en echelon R-shears always results in restraining geometries in the relay zones between shears (Figure 10c), and the shears are oriented about 15–25° from the bulk shear direction [*Casas et al.*, 2001; *Lowell*, 1972; *Wilcox et al.*, 1973; *Naylor et al.*, 1986]. En echelon R shears are observed along continental transform plate boundary faults, such at the San Andreas, but at lower angles (2–8°) than the models predict [*Wallace*, 1973; *Aydin and Schultz*, 1990]. Where P-shears dominate, the stepping direction always results in extensional relay zones between fault segments (Figure 10c). In analogue models and in the Carboneras fault system in SE Spain, en echelon P-shears are oriented about 12–27° to the bulk shear direction [*Keller et al.*, 1997].

[40] The en echelon faults along the Macquarie and McDougall segments of the MRC are oriented at ∼3–6° to the overall strike of the plate boundary at any given location, even though the plate boundary curves or changes orientation (Figure 4). This angular relationship is similar to the San Andreas example, but our faults step with the opposite sense, consistent with them having originated as P-shears. The faults are oriented about halfway between P-shears and plate boundary-parallel Y-shears (Figure 10c). One explanation could be that these faults represent P-shears that formed in response to transpression at the plate boundary and were subsequently rotated into a more plate boundary parallel orientation during subsequent deformation. However, this does not take into account the curvature of the plate boundary, and we suggest below that curvature is the dominant control on the en echelon pattern.

5.4. Model for Formation of Plate Boundary Faults

[41] Any model for formation of plate boundary faults along the MRC must explain the development of local extension across a zone which is clearly experiencing transpression. Three key observations are: 1) minor local extension associated with a few small right step-overs along the McDougall segment, 2) the development of a large right step-over and major local extension at the boundary of the McDougall and Macquarie segments, and 3) local extension on Macquarie Island that increases in intensity southward along the MRC.

[42] The present-day curvature of the plate boundary is inherited from the preexisting divergent plate boundary and has been modified very little since seafloor spreading stopped at ∼10 Ma (Figure 10a). We propose that when faults related to the right lateral transform formed, their orientation was controlled by the concave east curvature of the plate boundary, resulting in a series of straight, en echelon faults that step to the right to conform to the preexisting geometry (Figure 10b). The en echelon steps may develop as many small steps on a broad curve or as one big step at a significant change in orientation. The right steps in the plate boundary faults result in local extension in the transfer zone between fault segments.

[43] We infer that the degree of curvature in the plate boundary controls the length of fault segments and the number of en echelon steps. For example, the plate boundary, along the McDougall segment, shows minor curvature with a small change in strike (3–4°) distributed over the total length of the segment (curvature exaggerated in Figure 10b, true curvature shown in Figure 4). Such curvature requires a step to develop, on average, every 70–80 km so that this segment of the plate boundary divides into four relatively long en echelon faults linked by small extensional relay zones or pull-apart basins (≤500 m deep and 3.5 km wide). On the other hand, the Macquarie segment has a slightly sinuous plate boundary (Figure 4c) that forms a minor releasing bend geometry (exaggerated in Figure 10b, actual bend shown in Figure 4c) that may account for some local extension at the bend south of Macquarie Island. We suggest that most extension, however, which increases toward the south, is related to many short fault segments and a higher density of steps (on average every 30 km) caused by large curvature in the plate boundary along the contigu-

ous Hjort segment (Figure 10b). The en echelon step density decreases northward along the Macquarie segment away from the major bend in the contiguous Hjort segment.

[44] Finally, we note a sharp change in strike of the plate boundary at the transition between the McDougall and Macquarie segments. The major step-over developed where a large (~18°) change in strike of the plate boundary occurs over a short distance (<50 km). We observe a complex array of lineaments on the Macquarie segment south of the pull-apart basin (Figure 4b) that is most likely due to areal contraction associated with the kink in the plate boundary geometry, on the basis of the boundary element models of *Bilham and King* [1989].

5.5. Ridge Formation and Strain Partitioning

[45] We have examined the McDougall (~410 km) and Macquarie (~350 km) segments of the ~1500 km long MRC (Figures 1 and 2) in detail, where the plate boundary tracks along ridge crests. In these two segments the plate boundary region is dominated by a 30–50 km wide, 3–5 km tall ridge bordered to the east by a ~1–1.5 km deep trough (Figure 2). The two ridges are wider and higher than most elongate ridges along ridge-ridge transforms; such ridges are generally 1–7 km wide and less than 2 km high (e.g., ridges at the Blanco transform [*Embley and Wilson*, 1992]; Clipperton transform [*Pockalny*, 1997]; and Kane transform [*Pockalny et al.*, 1988]). Larger ridges characterize longer ridge-ridge offsets (~750–900 km) such as at the Romanche and Andrew Bain transforms [*Honnorez et al.*, 1991; *Searle et al.*, 1994; *Ligi et al.*, 2002].

[46] *DeMets et al.* [1994] NUVEL-1A Australian-Pacific relative motion vectors intersect the McDougall and Macquarie segments of the plate boundary at 5–10° and 10–20° respectively, indicating that the plate boundary is clearly experiencing right lateral transpression. Recent analysis of magnetic anomaly and fracture zone data on the eastern end of the Southeast Indian spreading ridge suggests that a microplate, the Macquarie plate, evolved at ~6 Ma (Cande and Stock, submitted manuscript, 2003). Macquarie-Pacific relative motion vectors intersect both the McDougall and Macquarie segments of the plate boundary at ~20°. Meckel et al. (submitted manuscript, 2003) propose that transpression along the Macquarie segment of the plate boundary is partitioned into a strike-slip component parallel to the boundary and a convergent component that dynamically supports broad flexure of the Australian and Pacific plates (wavelength on the order of 100 km, amplitude 3–5 km), accounting for much of the anomalous bathymetry. At least part of the anomalous bathymetry, however, may have formed prior to transpression when much of the plate boundary was defined by relatively long (>100 km) ridge-ridge transforms that linked short spreading centers (Figure 10a). Teleseismic evidence from the Macquarie segment overwhelmingly indicates strike-slip motion [*Frohlich et al.*, 1997; Meckel et al., submitted manuscript, 2003], consistent with an interpretation of partitioning of strain at the plate boundary. Furthermore, our detailed analysis of recent fault geometries and kinematics on Macquarie Island shows no evidence of recent thrust faults.

[47] Dynamically supported flexure causing anomalous bathymetry along the MRC may also explain local extension across the transpressional Australian-Pacific plate boundary. Flexure of the lithosphere should result in extensional strains at crustal depths above a neutral surface (Figure 10d), and contractional strains at crustal depths beneath a neutral surface. Such extension might contribute, at least in part, to the extension caused by the right stepping fault traces. Finally, any gravitational potential energy created by the MRC topography would cause horizontal extensional stresses near the highest point of the ridge complex. This may also contribute to extension as observed across the transpressional Australian-Pacific plate boundary.

[48] The concentrated zone of deformation associated with the transpressional Australian-Pacific oceanic transform plate boundary near Macquarie Island suggests that most strike-slip movement predicted by relative plate motions is accommodated on a single narrow fault zone, indicating a high degree of strike-slip partitioning between strike-slip faults and flexure of the lithosphere.

[49] Kinematic analyses of transpression at continental plate boundaries [*Teyssier et al.*, 1995] shows a quantitative relation among the angle of relative plate motion, instantaneous strain axes and strike-slip partitioning. With an angle of convergence of <20°, *Teyssier et al.* [1995] suggested that transpression will be wrench-dominated and that strike-slip partitioning is favored. Their results are consistent with our interpretation that the McDougall and Macquarie segments of the MRC, which have angles of convergence <20°, are wrench dominated and show a high degree of strike-slip partitioning. With convergence angles of >20°, *Teyssier et al.* [1995] suggest that transpression should be pure-shear dominated and involve little strain partitioning. In comparison, the northern boundary of the Easter microplate has convergence angles of >50° and shows a diffuse zone of thrust faults in the Nazca plate immediately north of the right-lateral transpressive plate boundary [*Rusby and Searle*, 1993], indicating pure-shear dominated deformation and low degree of strike-slip partitioning in oceanic crust. Thus these two examples suggest that the conclusions reached by *Teyssier et al.* [1995] in their study of continental plate boundary processes may be extended to the oceanic realm.

5.6. Comparison With Other Oceanic and Continental Transforms

[50] En echelon fault patterns, similar to those observed along the MRC, are a common geometry in strike-slip faults on all scales, and a fault zone may show both left and right senses of en echelon step along the one fault [*Aydin and Schultz*, 1990] (Figure 10c). For example, the San Andreas Fault in northern California is a right-lateral fault system with many left steps resulting in areas of uplift in contractional relay zones [e.g., *Wallace*, 1973]. On the other hand, the Dead Sea fault system is a left-lateral fault with many left steps resulting in areas of basin development in extensional relay zones [*Garfunkel*, 1981; *Garfunkel et al.*, 1981; *Garfunkel and Ben-Avraham*, 1996; *ten Brink et al.*, 1999]. Preexisting fault patterns, heterogeneity of lithology, changing boundary conditions and changes in relative plate motions control the sense of en echelon step.

[51] En echelon faults are also observed along oceanic transforms. Strike-slip motion is accommodated by a succession of pull-apart basins and spreading segments along the Australian-Pacific plate boundary north of New Zealand and the Tonga trench near to the Futuna-Alofi Islands, where both extensional and contractional jogs in the plate boundary have been described [*Pelletier et al.*, 2000]. Step-overs and pull-apart basins similar to those along the MRC characterize ridge-ridge transforms, such as the Cascadia and Gorda depressions along the Blanco transform [*Embley and Wilson*, 1992]. Also some step-overs at ridge-ridge transforms have been interpreted to contain short intratransform spreading centers, such as along the Siqueiros transform [*Fornari et al.*, 1989]. Recent changes in the pole of rotation for Juan de Fuca-Pacific plate motion are inferred to have controlled the development of the Blanco and Siqueiros step-over geometries as older parts of the transform fault realigned with the new relative plate motion vectors [*Embley and Wilson*, 1992; *Fornari et al.*, 1989]. The resolution of our data is not able to distinguish any evidence of recent volcanism in the McDougall-Macquarie depression, suggesting that it is probably more like the Blanco transform depressions. However, closer inspection of this zone may yet indicate volcanism in the Macquarie-McDougall depression.

6. Conclusion

[52] The Macquarie and McDougall segments of the Australian-Pacific transform plate boundary is comprised of a series of major en echelon, right lateral faults that step to the right, producing extensional relay zones and pull-apart basins (up to 10 km wide and 1.2 km deep) between fault tips where displacement is transferred. Subsidiary faults increase in number in the transfer zones and form smaller pull-apart basins accommodating local extensional stresses. The zone of associated deformation is 5–15 km wide.

[53] We propose that the preexisting curved plate boundary geometry controlled the orientation of the new right lateral transform faults when relative Australian-Pacific plate motion became dominantly

transform in the McDougall and Macquarie regions, and that they formed with right stepping en echelon geometry following the inherited curvature. We conclude that the degree of preexisting curvature or a large change in plate boundary orientation, such as between at the McDougall and Macquarie segments, control the density and size of en echelon steps along the plate boundary.

[54] Recent faulting on Macquarie Island reflects dominantly extensional tectonics, apparently in conflict with the island's transpressional tectonic setting and history of uplift. However, we infer that the island is located within an extensional local stress field related to right steps in the plate boundary located ~4.5 km to the west, and fault geometries and kinematics are not related to current transpression at the plate boundary.

[55] We propose that transpression at the plate boundary is partitioned into a strike-slip component parallel to the boundary, forming the en echelon strike-slip faults and a convergent component causing the anomalous bathymetric ridge and trough morphology of the McDougall and Macquarie segments of the MRC.

Acknowledgments

References

Alt, J. C., G. J. Davidson, D. A. H. Teagle, and J. A. Karson, Isotopic composition of gypsum in the Macquarie Island ophiolite: Implications for the sulfur cycle and the subsurface biosphere in oceanic crust, *Geology*, *31*, 549–552, 2003.

Aydin, A. A., and R. A. Schultz, Effect of mechanical interaction on the development of strike-slip faults with en echelon patterns, *J. Struct. Geol.*, *12*, 123–129, 1990.

Bernardel, G., and P. A. Symonds, Seafloor mapping of the south-east region and adjacent waters—AUSTREA final report: Southern Macquarie Ridge, *Rec. 2001/46*, 78 pp., Geosci. Australia, Canberra, Australian Capital Territory, Australia, 2001.

Bilham, R., and G. King, The morphology of strike-slip faults: Examples from the San Andreas Fault, California, *J. Geophys. Res.*, *94*, 10,204–10,216, 1989.

Cande, S. C., J. M. Stock, R. D. Mueller, and T. Ishihara, Cenozoic motion between East and West Antarctica, *Nature*, *404*, 145–150, 2000.

Casas, A. M., D. Gapais, T. Nalpas, K. Besnard, and T. Roman-Berdiel, Analogue models of transpressive systems, *J. Struct. Geol.*, *23*, 733–743, 2001.

Christodoulou, C., B. J. Griffin, and J. Foden, The geology of Macquarie Island, *Aust. Natl. Antarct. Res. Expeditions Res. Notes*, *21*, 1–15, 1984.

DeMets, C., R. G. Gordon, D. F. Argus, and S. Stein, Effect of recent revisions to the geomagnetic reversal time scale on estimates of current plate motions, *Geophys. Res. Lett.*, *21*, 2191–2194, 1994.

Duncan, R. A., and R. Varne, The age and distribution of the igneous rocks of Macquarie Island, *Pap. Proc. R. Soc. Tasmania*, *114*, 45–50, 1988.

Embley, R. W., and D. S. Wilson, Morphology of the Blanco Transform Fault Zone-NE Pacific: Implications for its tectonic evolution, *Mar. Geophys. Res.*, *14*, 25–45, 1992.

Fornari, D. J., D. G. Gallo, M. H. Edwards, J. A. Madsen, M. R. Perfit, and A. N. Shor, Structure and topography of the Siqueiros Transform Fault system: Evidence for the development of intra-transform spreading centers, *Mar. Geophys. Res.*, *11*, 263–299, 1989.

Frohlich, C., M. F. Coffin, C. Massell, P. Mann, C. L. Schuur, S. D. Davis, T. Jones, and G. Karner, Constraints on Macquarie Ridge tectonics provided by Harvard focal mechanisms and teleseismic earthquake locations, *J. Geophys. Res.*, *102*, 5029–5041, 1997.

Gallo, D. G., P. J. Fox, and K. C. Macdonald, A Sea Beam investigation of the Clipperton Transform Fault: The morphotectonic expression of a fast slipping transform boundary, *J. Geophys. Res.*, *91*, 3455–3467, 1986.

Garfunkel, Z., Internal structure of the Dead Sea leaky transform (rift) in relation to plate kinematics, *Tectonophysics*, *80*, 81–108, 1981.

Garfunkel, Z., and Z. Ben-Avraham, The structure of the Dead Sea basin, *Tectonophysics*, *266*, 155–176, 1996.

Garfunkel, Z., I. Zak, and R. Freund, Active faulting in the Dead Sea rift, *Tectonophysics*, *80*, 1–26, 1981.

Goscombe, B. D., and J. L. Everard, Geology of Macquarie Island, Geological Atlas1:10,000 Series, 7 sheets, Miner. Resour. of Tasmania, Hobart, Australia, 1998.

Goscombe, B. D., and J. L. Everard, Tectonic evolution of Macquarie Island: Extensional structures and block rotations in oceanic crust, *J. Struct. Geol.*, *23*, 639–673, 2001.

Hayes, D. E., and M. Talwani, Geophysical investigation of the Macquarie ridge complex, in *Antarctic Oceanology II: The Australian-New Zealand Sector*, *Antarct. Res. Ser.*,

vol. 19, edited by D. E. Hayes, pp. 211–234, AGU, Washington, D. C., 1972.

Honnorez, J., J. Mascle, C. Basile, P. Tricart, M. Villeneuve, and H. Bertrand, Mapping of a segment of the Romanche Fracture Zone: A morphostructural analysis of a major transform fault of the equatorial Atlantic Ocean, *Geology*, *19*, 795–798, 1991.

Karson, J. A., Variations in structure and petrology in the Coastal complex, Newfoundland: Anatomy of an oceanic fracture zone, in *Ophiolites and Oceanic Lithosphere*, edited by I. G. Gass, S. J. Lippard, and A. W. Shelton, *Geol. Soc. Spec. Publ.*, *13*, 131–144, 1984.

Kastens, K. A., W. B. F. Ryan, and P. J. Fox, Structural and volcanic expression of a fast slipping ridge-transform-ridge-plate boundary: Sea MARC I and photographic surveys at the Clipperton Transform Fault, *J. Geophys. Res.*, *91*, 3469–3488, 1986.

Keller, J. V. A., S. H. Hall, and K. R. McClay, Shear fracture pattern and microstructural evolution in transpressional fault zones from field and laboratory studies, *J. Struct. Geol.*, *19*, 1173–1187, 1997.

Keller, W. R., J. M. Stock, S. C. Cande, and R. D. Müller, Geophysical constraints on the plate tectonic history of the Emerald Basin and South Tasman Ocean Crust southwest of New Zealand, *Eos Trans. AGU*, *83*(47), Fall Meet. Suppl., abstract T52A-1185, 2002.

Lamarche, G., J.-Y. Collot, R. A. Wood, M. Sosson, R. Sutherland, and J. Delteil, The Oligocene-Miocene Pacific-Australia plate boundary, south of New Zealand: Evolution from oceanic spreading to strike-slip faulting, *Earth Planet. Sci. Lett.*, *148*, 129–139, 1997.

Ligi, M., E. Bonatti, L. Gasperini, and A. N. B. Poliakov, Oceanic broad multifault transform plate boundaries, *Geology*, *30*, 11–14, 2002.

Lowell, J. D., Spitsbergen Tertiary Orogenic Belt and the Spitsbergen Fracture Zone, *Geol. Soc. Am. Bull.*, *83*, 3091–3102, 1972.

Massell, C., M. F. Coffin, P. Mann, S. Mosher, C. Frohlich, C. S. Duncan, G. Karner, D. Ramsay, and J.-F. Lebrun, Neotectonics of the Macquarie Ridge Complex, Australia-Pacific plate boundary, *J. Geophys. Res.*, *105*, 13,457–13,480, 2000.

Mitchell, N. C., Seafloor slopes at mid-ocean ridges from submersible observations and implications for interpreting geology from seafloor topography, *Earth Planet. Sci. Lett.*, *183*, 543–555, 2000.

Naylor, M. A., G. Mandl, and C. H. K. Sijpesteijn, Fault geometries in basement-induced wrench faulting under different initial stress states, *J. Struct. Geol.*, *8*, 737–752, 1986.

Pelletier, B., Y. Lagabrielle, G. Cabioch, S. Calmant, M. Régnier, and J. Perrier, Active transpression along the fast Pacific-Australian transform boundary revealed by swath mapping around the Futuna-Alofi Islands, *C. R. Acad. Sci., Ser. II*, *331*, 127–132, 2000.

Pockalny, R. A., Evidence of transpression along the Clipperton Transform: Implications for processes of plate boundary reorganization, *Earth Planet. Sci. Lett.*, *146*, 449–464, 1997.

Pockalny, R. A., R. S. Detrick, and P. J. Fox, Morphology and tectonics of the Kane Transform from Sea Beam bathymetry data, *J. Geophys. Res.*, *93*, 3179–3193, 1988.

Rusby, R. I., and R. C. Searle, Intraplate thrusting near the Easter microplate, *Geology*, *21*, 311–314, 1993.

Searle, R. C., M. V. Thomas, and E. J. W. Jones, Morphology and tectonics of the Romanche Transform and its environs, *Mar. Geophys. Res.*, *16*, 427–453, 1994.

Simonian, K., and I. G. Gass, Arakapas fault belt, Cyprus, a fossil transform fault, *Geol. Soc. Am. Bull.*, *89*, 1220–1230, 1978.

Sutherland, R., and R. J. Norris, Late Quaternary displacement rate, paleoseismicity, and geomorphic evolution of the Alpine Fault: Evidence from Hokuri Creek, South Westland, New Zealand, *N. Z. J. Geol. Geophys.*, *38*, 419–430, 1995.

Sylvester, A. G., and R. R. Smith, Tectonic transpression and basement-controlled deformation in San Andreas Fault Zone, Salton Trough, California, *AAPG Bull.*, *60*, 2081–2102, 1976.

ten Brink, U. S., M. Rybakov, A. S. Al-Zoubi, M. Hassouneh, U. Frieslander, A. Batayeneh, V. Goldschmidt, M. N. Daoud, Y. Rotstein, and J. K. Hall, Anatomy of the Dead Sea transform: Does it reflect continuous changes in plate motion?, *Geology*, *27*, 887–890, 1999.

Teyssier, C., B. Tikoff, and M. Markley, Oblique plate motion and continental tectonics, *Geology*, *23*, 447–450, 1995.

Varne, R., and M. J. Rubenach, Geology of Macquarie Island and its relationship to oceanic crust, in *Antarctic Oceanology II: The Australian-New Zealand Sector*, *Antarct. Res. Ser.*, vol. 19, edited by D. E. Hayes, pp. 251–266, AGU, Washington, D. C., 1972.

Varne, R., R. D. Gee, and P. J. Quilty, Macquarie Island and the cause of oceanic linear magnetic anomalies, *Science*, *166*, 230–232, 1969.

Varne, R., A. V. Brown, and T. Falloon, Macquarie Island: Its geology, structural history, and the timing and tectonic setting of its N-MORB to E-MORB magmatism, in *Ophiolites and Oceanic Crust: New Insights From Field Studies and the Ocean Drilling Program*, edited by Y. Dilek et al., pp. 301–320, Geol. Soc. of Am., Boulder, Colo., 2000.

Wallace, R. E., Surface fracture patterns along the San Andreas Fault, in *Proceedings of the Conference on Tectonic Problems of the San Andreas Fault System*, edited by R. L. Kovach and A. Nur, pp. 248–250, Stanford Univ. Press, Stanford, Calif., 1973.

Wertz, K. L., S. Mosher, N. R. Daczko, and M. F. Coffin, Macquarie Island's Finch-Langdon fault: A ridge-transform inside-corner structure, *Geology*, *31*, 661–664, 2003.

Wilcox, R. E., T. P. Harding, and D. R. Seely, Basic wrench tectonics, *AAPG Bull*, *57*, 74–96, 1973.

Wood, R., G. Lamarche, R. Herzer, J. Delteil, and B. Davy, Paleogene seafloor spreading in the southeast Tasman Sea, *Tectonics*, *15*, 966–975, 1996.